coatings

MDPI

Article

Multifunctional Properties of PBAT with Hemp (*Cannabis sativa*) Micronised Fibres for Food Packaging: Cast Films and Coated Paper

Hafsae Lamsaf [1], Srishti Singh [1], Joel Pereira [2] and Fátima Poças [1,2,*]

[1] Universidade Católica Portuguesa, CBQF—Centro de Biotecnologia e Química Fina—Laboratório Associado, Escola Superior de Biotecnologia, Rua Diogo Botelho 1327, 4169-005 Porto, Portugal; hafsae.lamsaf@gmail.com (H.L.); ssingh@ucp.pt (S.S.)
[2] Centre for Food Quality and Safety, Escola Superior de Biotecnologia, Universidade Católica Portuguesa, Rua Diogo Botelho 1327, 4169-005 Porto, Portugal; jppereira@ucp.pt
* Correspondence: fpocas@ucp.pt

Abstract: Hemp (*Cannabis sativa*) stalk fibres from industry residues were incorporated into polybutylene adipate terephthalate, a synthetic biodegradable polyester, to produce films and paper coatings. The lignocellulosic components and the chemical composition of the fibres were analysed, and the results highlight the bioactivity due to cannabinoids, alkanoids, and lignin, among others, making the fibres attractive for active food packaging. The incorporation, without chemical modification, of 2% (*w*/*w*) hemp in the PBAT matrix increased the water vapour permeability of PBAT around 22%. The impact on mechanical properties was determined, and the results show that the PBAT/hemp film is less stretchable but stronger than the pure PBAT film. The incorporation of hemp enhanced significantly the compostability of PBAT. The PBAT/hemp films and paper coatings composted two times faster than those using pure PBAT.

Keywords: hemp fibres; PBAT; compostable; food packaging; active packaging

Citation: Lamsaf, H.; Singh, S.; Pereira, J.; Poças, F. Multifunctional Properties of PBAT with Hemp (*Cannabis sativa*) Micronised Fibres for Food Packaging: Cast Films and Coated Paper. *Coatings* **2023**, *13*, 1195. https://doi.org/10.3390/coatings13071195

Academic Editor: Maria Jose Fabra

Received: 4 June 2023
Revised: 25 June 2023
Accepted: 27 June 2023
Published: 3 July 2023

1. Introduction

Hemp is considered one of the oldest cultivated plants in human history (8000 BC). Hemp seed and oil were used first in the Central Asia, then Europe, Africa, and South of America [1]. Between 2015 and 2019, hemp production increased by more than 60%. The leading producer countries are France, with more than 70% of the EU's production, the Netherlands (10%), and Austria (4%). During the last few decades, a huge interest in cannabis derivatives has arisen in Portugal where the weather conditions allow for the production of well-valued fibres. Hemp stalks are considered an important by-product of the hemp industry. The fibres of hemp have high strength, a high Young's modulus, and an interesting concentration of cellulose compared with other plants [2]. Their potential bioactivity, due to its composition in cannabinoids, alkaloids, and lignin, among other substances, makes them very attractive for food packaging [3].

Packaging for food consumes an important fraction (around 40%) of all plastic materials [4]. Food packaging is critical for extending the food shelf-life, maintaining the quality and safety, therefore, preventing food losses and waste. Plastics have a set of overall performance properties difficult to match [5]. However, due to the well-known end-of-life problems of plastics, different measures have been implemented, and the European Commission announced in 2018 an ambitious plan to prevent and minimize plastic waste in Europe. This strategy includes specific actions, such as banning single-use plastic items that are most frequently released in the environment and found on European beaches, and other articles that come into contact with food, such plastic straws, plates, and cutlery. Food companies are therefore switching to substitutes that are either made of cellulose or perceived as sustainable solutions [6].

Improving the functional properties of the materials with active and smart systems and the use of biodegradable packages in specific applications are approaches that can contribute to decrease food and plastic waste [7]. Polybutylene adipate terephthalate (PBAT) and its blends and composites are promising biodegradable polymers due to their good resistance to water and mechanical flexibility compared with other biopolymers such as polylactic acid (PLA) and poly(butylene-co-succinate) (PBS) [8]. When compared with other fossil-based plastics, PBAT is still relatively high-cost and has weak properties related to moisture barrier, thermal stability, and mechanical resistance [9,10]. Today, PBAT is commonly used in packaging for short time of contact, agricultural films, and as compostable bags [11]. It is used blended with other compounds such as PLA, poly(3-hydroxybutyric acid-co-3-hydroxyvaleric acid (PHBV), and starch to improve its mechanical properties profile and to decrease the cost of the final material [10].

Recently, research has focused on the improvement of PBAT properties by the incorporation of organic compounds, such as starch nanoparticles [12] and, nanocrystalline cellulose [13], and inorganic components such as titanium and zinc oxides, into films [14]. Many works have focused on combining PBAT with functional substances to design composites to be exploited in the food packaging industry, such as essential oils and phenolic compounds of different plants [15], approved preservatives such as nisin and sorbate or benzoate [16,17], and combinations with lignin [18]. The high cost of PBAT can be lowered by modifying PBAT composites with low-cost materials and food industry residues. Torrefied coffee grounds were used to reinforce PBAT composite and resulted in better hydrophobicity and thermo-mechanical properties [19]. The results for nanocomposite blown films based on PBAT and layered silicate have shown improved tensile properties, thermal stability, and biodegradation rates [20]. Clay was blended into PBAT films in order to improve their mechanical characteristics; in particular, their hardness and Young's modulus [21], thermal stability, and water vapour barrier [10,22].

Hemp fibres have shown strengthening behaviour for composites with other polyesters [23] and with polypropylene [24], affecting, specifically, thermal degradation and surface energy. PBAT also showed enhancement of thermo-mechanical properties when reinforced with hemp fibres after chemical treatment [10,25]. Composite properties depend on the interfacial adhesion between the polymer and the lignocellulosic fibre, which is influenced by the surface chemistry of the fibres and the polarity of the polymer. Modification of hemp fibres with silane improved the interface interaction between the fibres and PBAT, resulting in better tensile properties [26]. The chemical characteristics of the fibre per se is also an important factor, especially when unmodified fibres are incorporated. The incorporation of hemp into a PBS polymeric matrix showed better mechanical properties in comparison with other plant fibres such as kenaf or jute, which was due to the better interfacial adhesion with fibres with low lignin content, such as hemp [27].

Regarding sustainable alternatives for food packaging and the replacement of plastics in some applications, paper and other cellulosic-based materials are receiving an exponentially increasing amount of interest at research and industry levels. However, the barrier and mechanical characteristics of these materials must be improved to meet food protection, safety, and shelf-life requirements. Coatings of PBAT and its blends or composites are promising to enhance the barrier properties [28,29] of cellulosic-based packaging and for other applications, such as pressure sensors [30] and highly sensitive medical analysis devices [31].

In the present work, PBAT incorporated with unmodified hemp micronised fibres was used to produce films by solvent casting and paper coatings for packaging. The hemp fibres, the film, and the coated paper were characterised with regard to their morphology and functional properties, i.e., thermal, mechanical, and barrier properties. Many studies on the incorporation of fibres in PBAT have been reported, but the chemical aspects are not often addressed. In this work, the chemical composition of the film with hemp fibres and the active components are reported. The end-of-life of these materials was also addressed, and compostability was tested.

2. Materials and Methods

2.1. Raw Materials

PBAT pellets (Ecoflex® F blend C1200, BASF, Lemförde, Germany) were provided by a local converter.

The hemp (*Cannabis sativa*) residue was grown in Portugal and supplied by a local converter. The fibres were obtained from micronised stalks by stone-milling (MagAger, Aguda, Portugal) and were sieved (<32 µm) before use.

White kraft paper with a GSM of 75 g m^{-2} and a thickness 85 µm (Billerud AB, Sweden) was supplied by a local converter (EMBA—Comércio e Indústria de Embalagem, SA, Alenquer, Portugal).

2.2. Material Production

The PBAT-based materials were prepared via solvent casting for the preparation of films and via bar-coating of an organic suspension to obtain coated paper. Materials were prepared with PBAT and with PBAT/hemp-fibre mixtures.

2.2.1. Cast Films

The self-standing films were produced by solvent casting as indicated in Figure 1. PBAT pellets (10 g) were dissolved in 150 mL chloroform (99.0% pure, Merck, Darmstadt, Germany). For the PBAT/hemp materials, a solution of 2% (*w*/*w*) hemp was prepared in the PBAT matrix. Higher concentrations were tried with poorer results for surface morphology. Modification of PBAT is needed to increase the interfacial interaction to an extent that allows for the incorporation of high levels of the organic phase, such as starch or hemp. The objective of the work was to study the incorporation of unmodified hemp. Therefore, a low level of incorporation was used.

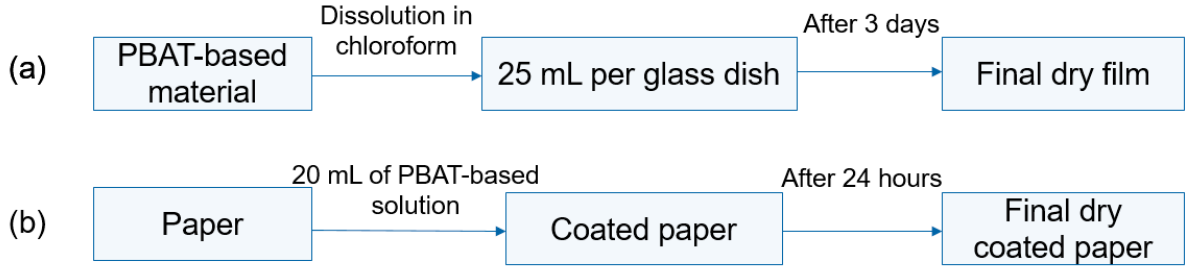

Figure 1. Preparation of (**a**) cast films and (**b**) coated paper with PBAT and PBAT/hemp.

The solutions were stirred for 2 to 3 h at room temperature until complete dissolution was achieved. Twenty-five mL of each solution was poured into glass petri dishes of 9 cm^2 diameter and left for the solvent to evaporate at room temperature. The films were then removed from the petri dishes and conditioned at 23 °C and 50% relative humidity before characterisation and testing.

2.2.2. Coated Paper

The same solutions of PBAT and PBAT/hemp described in Section 2.2.1. were used for coating the paper using an automatic coating bar applicator (TQCSHEEN, Capelle aan den IJssel, The Netherlands). The opening of the coating slit was 90 µm thick, with a width of 10 cm and a coating speed of 100 mm s^{-1}. Figure 1 illustrates the process.

2.3. Characterisation

Hemp fibre morphology was characterised using scanning electron microscopy (SEM, Thermo Fischer Scientific—FEI, Eindhoven, The Netherlands). Chemical analyses were performed to determine the lignocellulosic components and the volatile and semi-volatile components. Elemental analysis was performed by energy-dispersive X-ray spectroscopy.

PBAT-based cast films and coatings were characterised with regard to their morphology, thermal transitions, water vapour permeability, mechanical properties, colour, and compostability. The infra-red spectra were also obtained.

2.3.1. Morphology

SEM was used to analyse the morphology of samples (Phenom XL G2 by Thermo Fischer Scientific—FEI, Eindhoven, Netherlands) with SED and BSED detectors (acceleration voltage of 5 keV and magnification of X500 for fibres and X3000 for film images). The samples were coated with a gold layer in a polaron sputter coater (Quorum Technologies Ltd, Lewes, UK) for 1 min with a current of 20 mÅ in the presence of argon. The ImageJ software (version v1.54d) [32] was used to analyse the data collected of the material surface and of the fibres.

2.3.2. Lignocellulosic Components

The concentration of cellulose, hemicellulose, and lignin in hemp fibres was estimated by solvent extraction and gravimetry as proposed by [33] and as described in the literature [34]. Chemicals used were 99.8% pure acetone (Merck, Darmstadt, Germany), 98% sulphuric acid (Merck), pure solid sodium hydroxide (Supelco, Algés, Portugal), and barium chloride (Merck).

2.3.3. GC-MS Screening

The screening of hemp fibres was performed using the gas chromatography–mass spectroscopy system (GC-MS), GC456 (Bruker, Coventry, UK) connected to a triple quadrupole SCION TQ (MS) mass spectrometer (Scion Instruments, Bremen, Germany) and an automatic injector Combi-pal (CTC Analytics, Zwingen, Switzerland). The sample was treated by liquid extraction (LE) before analysis: 10 g of sample was extracted with 60 mL of a mixture of hexane and acetone 50/50 (v/v) for 24 h at 60 °C, following concentration under nitrogen flux. The injection volume was 1 mL in splitless mode (injector temperature of 300 °C) and the temperature program was 40 °C for 2 min, increasing at 10 °C min^{-1} to 320 °C for 25 min. The separation column used was 30 m × 0.25 mm with a 0.25 µm BR5 ms phase. The injector temperature was 250 °C. Helium was used as the carrier gas (1 mL min^{-1}) and the MS detector was run in scan mode from 43 to 330 m/z and operating at an EI of 70 eV. The analyses were performed in duplicate.

2.3.4. Elemental Analysis

Elemental analysis was performed by energy-dispersive X-ray spectroscopy (EDS)-mapping in transmission mode. Spectra were acquired using a double-corrected Titan Themis (Thermo Fisher, Eindhoven, The Netherlands) operated at 200 keV and equipped with a Super-X EDS detector.

2.3.5. Thermal Transitions

The glass transition temperature (Tg), melting temperature (Tm), and crystallisation temperature (Tc) were determined according to the standard ASTM D3418 by differential scanning calorimetry (DSC 204 F1 Phoenix by Netzsch, Germany). The tests were performed in the following conditions: initial temperature of −50 °C and heating rate 10 mL min^{-1} to a final temperature of 250 °C. Determinations were made in the second heating cycle.

2.3.6. Water Vapour Permeability (WVP)

The water vapour transmission rate (WVTR) and the WVP were determined gravimetrically at 23 ± 3 °C and 50% relative humidity (RH) in accordance with the standard ASTM E-96.

2.3.7. Mechanical Properties

The tensile properties of PBAT films and paper (uncoated and coated) were measured (Testometric Co, Rochdale, UK) at the following conditions according to the standard ASTM D882 and analysed by winTest™ analysis 5.029 software: load cell was 5 KN and the speed was 500 mm min^{-1}. The testing specimens were rectangular (5.0 cm × 1.5 cm) and were conditioned at 23 ± 2 °C and 50 ± 5% RH before testing.

2.3.8. Optical Properties

Colour was analysed with a colorimeter CR 400 (Minolta, NY, USA) calibrated with a white standard colour plate used as a background for colour measurements (L^*, a^*, b^*). The opacity of the coatings, expressed as a percentage (%), was calculated by the Hunter lab method, using the ratio of the opacity of each sample on a black standard (Yb) and a white standard (Yw), as described [35].

2.3.9. Compostability

Compostability of PBAT-based cast films and coated paper was assessed as specified in the standards EN 13432 and ASTM D6400. The weight loss of samples buried in soil (Substrato Biológico Universal, Maia, Portugal) at 60 °C and 65% RH was monitored. The morphology, thermal transitions, and infra-red (IR) spectra of the films exposed to soil for different times were measured to monitor the degradation.

2.3.10. FTIR Spectroscopy

The IR spectra were determined using a PerkinElmer Spectrum 100 FT-IR Spectrometer (PerkinElmer, Buckinghamshire, UK) attached to a DTSG detector, with a measurement resolution of 4 cm^{-1}. Spectra were recorded in the range of 4000 and 600 cm^{-1} and comprised 32 co-added scans in Attenuated Total Reflectance (ATR) with a diamond w/ZnSe lens single reflection plate and PIKE. These were processed using Microsoft Excel.

2.3.11. Statistical Analyses

Data handling and analysis was performed using Microsoft Excel software (Excel version 2202, Redmond, WA, USA). When applicable, one-way ANOVA with a p-value indicating the probability of significance of <0.05 was used to verify statistically significant differences with SPSS Statistics 21 software (IBM SPSS Statistics version 28.0.0.0 (190), IBM Corporation, Armonk, New York, NY, USA).

3. Results and Discussion

3.1. Hemp Characterisation

The hemp fibre morphology and composition are discussed in the following sections.

3.1.1. Morphology

Figure 2 exhibits the morphology of the hemp fibres observed by SEM. The fibres present a relative heterogenous surface area, pore structure, and pore size, with length ranging from 12–220 µm, which is considered suitable to produce cast films from polymeric materials with a target thickness of around 260 µm. This heterogenicity could be expected as the fibres were not chemically treated and were only micronised by stone-milling.

3.1.2. Lignocellulosic Components

The percentage of the main lignocellulosic components of the fibres obtained from hemp stalks was estimated. As expected, cellulose was the component in the highest amount with 52%, followed by hemicellulose (43%) and lignin (5%). The method used did not allow pectin to be distinguished.

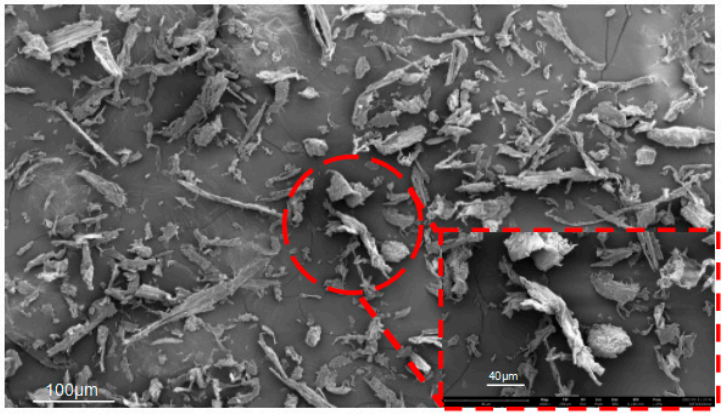

Figure 2. SEM image of hemp fibres (5 keV, magnification ×300; zoomed magnification of ×2000).

Hemp fibres are generally composed of 53%–91% cellulose, 4%–18% hemicellulose, 1%–17% pectin, and 1%–21% lignin (wt%) [36]. Cellulose is considered the most interesting component, as it can be used in the production of paper and incorporated into other packaging materials [34]. Higher values, around 70%, for the cellulose percentage in hemp have been reported in the literature [2], although with varying values, depending on the part of the plant (leaves, stem, and roots) [34]. Most of the literature presents values for the stems and not for the stalks. Additionally, different compositions may be found according to the cultivar [36].

3.1.3. GC-MS Screening for Bioactive Components

The bioactive components of hemp fibre were screened, and several techniques to treat the sample for gas-chromatography analysis were previously tested: headspace, solid-phase micro extraction, and liquid extraction. The latter was shown to produce better results, highlighting more components of the fibres. Therefore, only the results obtained by this technique are discussed. Figure 3 presents the GC-MS chromatogram of the liquid extracts of hemp fibres, and the compounds are identified in Table 1.

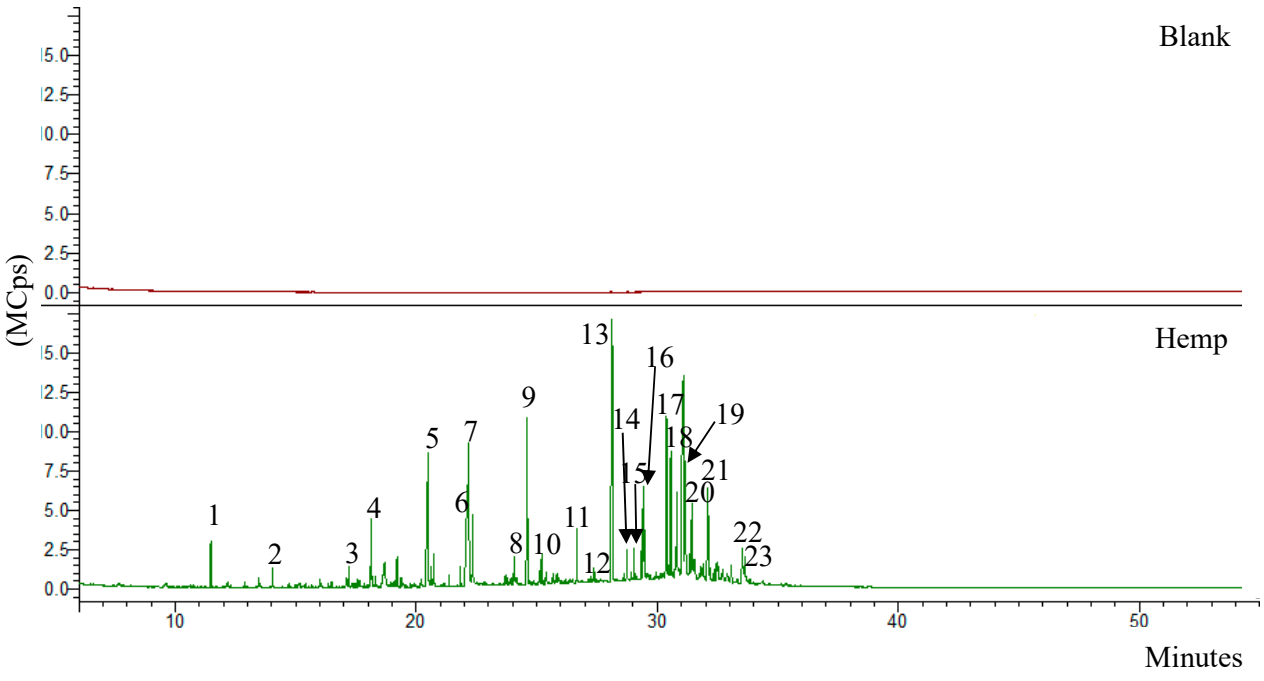

Figure 3. GC-MS chromatogram of hemp fibres after liquid extraction.

Table 1. Compounds detected in the hemp fibres by GC-MS after liquid extraction.

Peak	CAS	Name of Compound
1	496-16-2	2,3-dihydro-benzofuran
2	121-33-5	Vanillin
3	134-96-3	4-hydroxy-3,5-dimethoxy-benzaldehyde
4	32811-40-8	Trans-coniferyl alcohol
5	57-10-3	n-hexadecanoic acid
6	60-33-3	Linoleic acid
7	112-80-1	Oleic Acid
8	506-30-9	Eicosanoic acid
9	20675-51-8	Cannabichromene
10	54002-78-7	Related to Cannabielsoin
11–14, 16	593-49-7	Saturated alkanes
15	22725-64-0	Octacosanal
17	474-62-4	Campesterol
18	83-48-7	Stigmasterol
19	83-47-6	γ-sitosterol
20	20817-72-5	Stigmastadienone
21	84924-96-9	γ-Sitostenone
22	123-28-4	Didodecyl 3,3′-thiodipropionate
23	22149-69-5	Stigmastane-3,6-dione

More than 130 compounds were detected, and those of more relevant interest are listed in Table 1.

A variety of bioactive chemicals was detected with reported antimicrobial and antioxidant activities that can improve the properties of the PBAT matrix for packaging. Essential oils, phytosterols, terpenes, fatty acids, and cannabidiols were detected in similar quantities to published studies [37–39]. The presence of these bioactive compounds highlights the richness of the fibres and their potential application as active packaging for food. The full list of compounds detected by the different sample treatment techniques is presented in the Supplementary Information (Table S1).

3.1.4. Elemental Analysis

The EDS spectrum showed the hemp fibre elemental composition: carbon (68.7%), oxygen (13.7%), and a high percentage of aluminium (16.0%), followed by minor elements such as magnesium, silica, and potassium with a content lower than 1.0%. The aluminium content found is relatively high, although it may be expected as this varies with the part of the plant. This was discussed previously for cannabis leaves and their associated smoke [40], but much lower contents were detected. However, no other studies on the stalks were reported for comparison. Aluminium in packaging and food contact materials is relevant for food safety because it can migrate into food [41]. In 2008, the European Food Safety Authority (EFSA) set the provisional tolerable weekly intake value for aluminium at 1 mg kg^{-1} body weight per week [42,43]. It is thus recommended to test the migration of aluminium from materials with hemp fibre incorporated.

3.2. Characterization of PBAT/Hemp Materials

PBAT films with the incorporation of hemp fibres at 2% (*w*/*w*) and their respective paper coatings were analysed for morphology, thermal transitions, permeability to moisture, mechanical properties, and compostability in comparison with the neat PBAT (without incorporation of fibres).

3.2.1. Morphology

The surface morphology of pure PBAT and PBAT/hemp films are presented in Figures 4a and 4b respectively. The PBAT/hemp films showed a smoother surface compared to the pure PBAT, with homogeneous pore sizes (2–6 μm) of quasi-spherical

shape. The pores are due to air trapped in the matrix due the dissolution and casting steps. The hemp clusters crossed the outer layer of the film, making holes located in the centre of the film layer (Figure S1). The images show good adhesion between the fibres and the PBAT matrix.

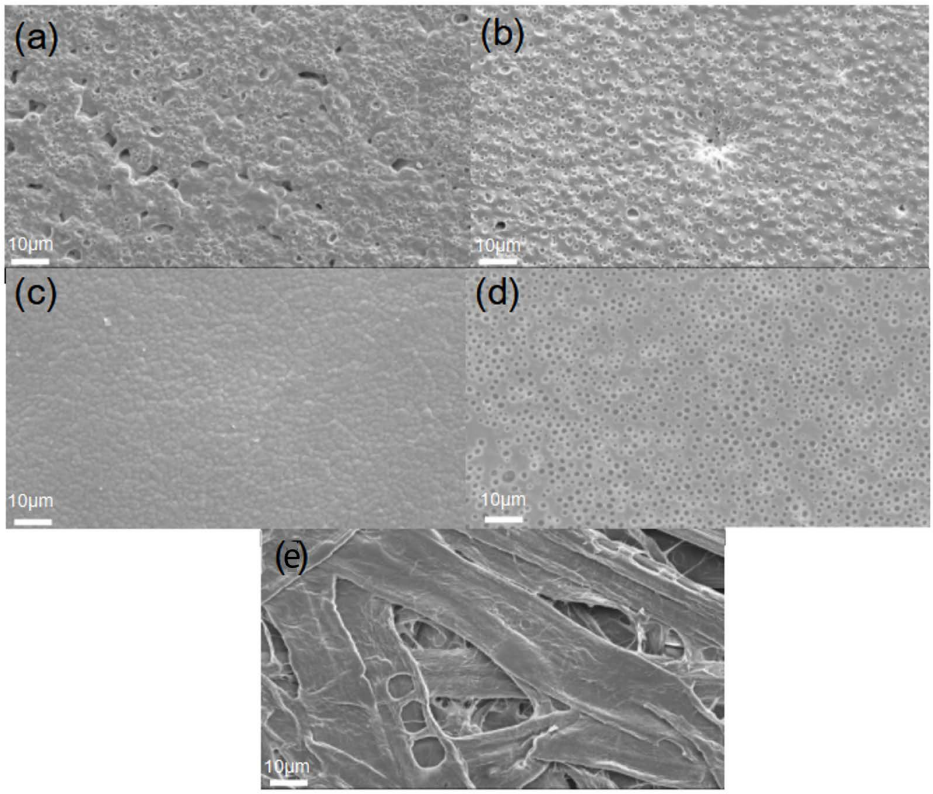

Figure 4. SEM images of cast film and coated paper: (**a**) PBAT cast film, (**b**) PBAT/hemp cast film, (**c**) PBAT coated paper, (**d**) PBAT/hemp coated paper, and (**e**) uncoated paper.

Figure 4c,d present the SEM images of paper coated with PBAT and PBAT/hemp. Uncoated paper presented the typical roughness characteristic of the individual fibres (Figure 4f). When coated, the surface of paper was totally covered by the PBAT matrix and similar morphology of the coated surface was found in the cast films, although a more uniform and smooth aspect could be observed. This could be expected because of the relative orientation effect that the coating bar may have on the surface of the wet coating. A partial penetration of the coating matrix in the paper fibre network could be observed, which is expected to improve the barrier properties because of the paper pore-blocking effect [44].

3.2.2. Thermal Transitions

The temperature of the thermal transitions was measured in the second heating cycle. The first heating cycle is aimed at removing the trapped humidity from the samples and to erase the memory of the polymer [45]. The DSC thermograms are presented in Figure 5. Table 2 displays the transition temperatures of the pure PBAT and PBAT/hemp films.

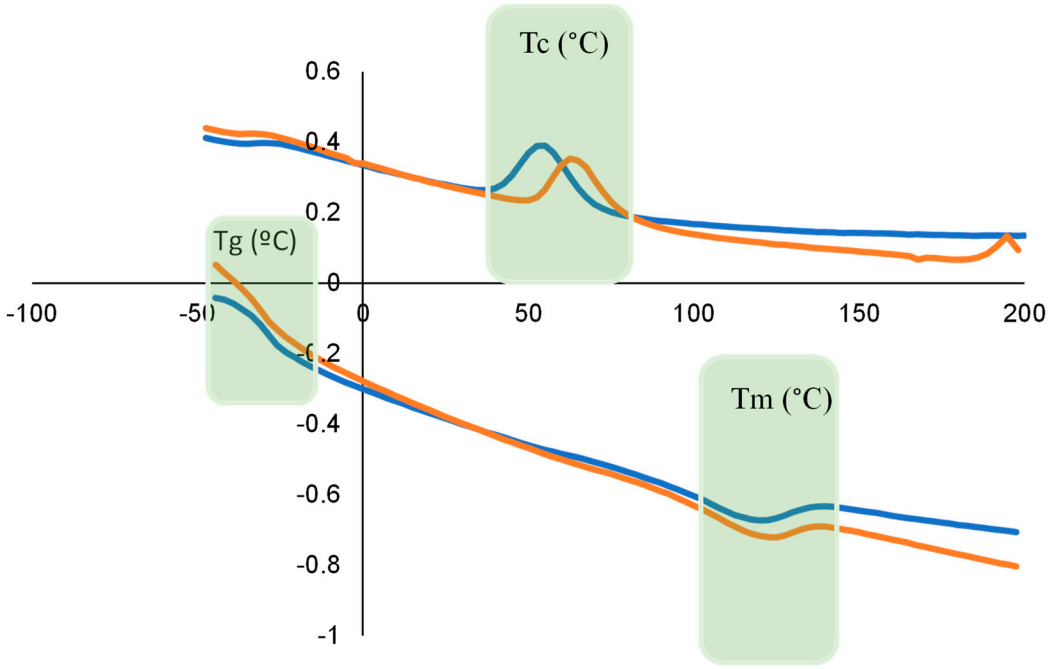

Figure 5. Thermogram of cast films (■ PBAT; ■ PBAT/hemp), where Tc is the crystallisation temperature, Tg is the glass transition temperature, and Tm is the melting temperature.

Table 2. Thermal transition of films.

Sample	Tg (°C)	Tc (°C)	Tm (°C)
PBAT	−27.3	53.9	120.6
PBAT/hemp	−31.1	63.3	124.1

The melting temperature of the material increases with the incorporation of the hemp fibres (from 120.6 to 124.1 °C) due to additional linkages by the reinforcement of the fibres and the possible presence of impurities. The glass transition temperature is usually seen to decrease in the presence of plasticisers or impurities and thus also happens with the incorporation of the fibres (−27.3 to −31.1 °C). These results agree with previously reported studies that found an increase in Tm from 121.9 to 125 °C with the incorporation of 10% hemp into PBAT films; however, there was a non-significant slight increase in Tg as determined by DSC [46].

The crystallisation temperature (Tc) increases from 53.9 °C in neat PBAT to 63.3 °C in the PBAT/hemp film, indicating higher crystallinity or a more compact structure, in agreement with the morphology results. Literature reporting a study with the addition of 10% coffee grounds also found a Tc increase from 76.8 °C to 85 °C [19]. This result confirms that the hemp fibres act as nucleation agents and constitute crystallisation centres for the polymeric matrix; consequently, the materials started to crystallise at a higher temperature upon cooling [47].

3.2.3. Water Vapour Permeability (WVP)

The water vapour permeability of a material is affected by various factors, particularly the composition, morphology, temperature, and relative humidity [48]. The WVTR is additionally affected by the thickness and by the permeation driving force, i.e., the vapour partial pressure difference between the two faces of the film. The WVP is normalised by these two factors. The value for the water saturation vapour pressure considered was 2.814 KPa at 23 °C.

The thickness of the films produced is presented in Table 3. The results show a slight effect of the hemp fibres on the WVP. The PBAT/hemp film WVP is 3633 (±56) g µm

m^{-2} day^{-1} KPa^{-1} while WVP of PBAT neat film is 2905 (±268) g µm m^{-2} day^{-1} KPa^{-1}. This indicates an increase in WVP, and thus, a relatively lower barrier to moisture, upon incorporation of the hemp fibres. This decrease in the barrier properties could be explained by the hydrophilic character of the untreated hemp fibres and by the structural changes of the PBAT/hemp film mentioned earlier under SEM analysis. The WVP value for the PBAT neat films is consonant with the values found in the literature, albeit slightly higher as could be expected because the films were casted and not extruded. The results indicate the obtained film could be used for food package applications, especially for breathable goods packaging [49].

Table 3. Thickness of the films produced.

Method	Material	Total Thickness (µm)
Casting	Pure PBAT	180 ± 19
	PBAT/hemp	173 ± 15
Coating	Pure paper	85 ± 2
	Paper/PBAT	144 ± 2
	Paper/PBAT/hemp	159 ± 3

The effect of coating on the barrier of paper to moisture agrees with the results obtained for the PBAT and PBAT/hemp films, as expected. In this case, the results are discussed as the WVTR because of the bi-material nature of the testing sample. The uncoated paper showed a value of WVTR of 496 (±16) g m^{-2} day^{-1}, measured at 23 °C and 50% relative humidity, which corresponds to ca. 31,000 g µm m^{-2} day^{-1} KPa^{-1}. The WVTR of PBAT-coated paper decreases to 45 (±6) g m^{-2} day^{-1}, and when coated with the PBAT/hemp, it decreases to 55 (±11) g m^{-2} day^{-1}. Therefore, the same effect of slightly decreasing the moisture barrier is observed when hemp is incorporated into PBAT for coating.

3.2.4. Mechanical Properties

Figure 6 presents the mechanical properties of cast films (PBAT and PBAT/hemp) and of the paper coated by the same materials. The results for uncoated paper and for paper treated with chloroform are also presented for comparison. Chloroform is the solvent used to dissolve and apply the PBAT and PBAT/hemp coatings. The incorporation of hemp into the PBAT layer increases the Young's modulus (Y) in the cast film and in the coating applied to paper (Figure 6a), although not significantly ($p < 0.05$). This could be explained by the inter-hydrogen molecular interaction between PBAT and the OH bond in the hemp fibres that contributes to an increase in Y, as reported earlier [50]. Wetting the paper by chloroform during the coating operation decreases Y. This effect has already been observed in paper with solution or dispersion coatings applied by casting at a laboratory scale, but it does not represent well the industrial applicators where solvent removal by drying is much faster. The stress at break does not change significantly ($p < 0.05$) with the incorporation of hemp fibres into both cast film and coated paper (Figure 6c). However, strain decreases upon the addition of hemp fibres to cast film, which can be explained by the presence of fibres in the polymeric layer (Figure 6b). This effect was not found in coated paper, which coincides with a previous study on coated paper/chitosan that reported no significant difference in mechanical properties [51]. The fracture energy of the coated paper samples shows an increase ($p < 0.05$) in the presence of hemp fibre (Figure 6d).

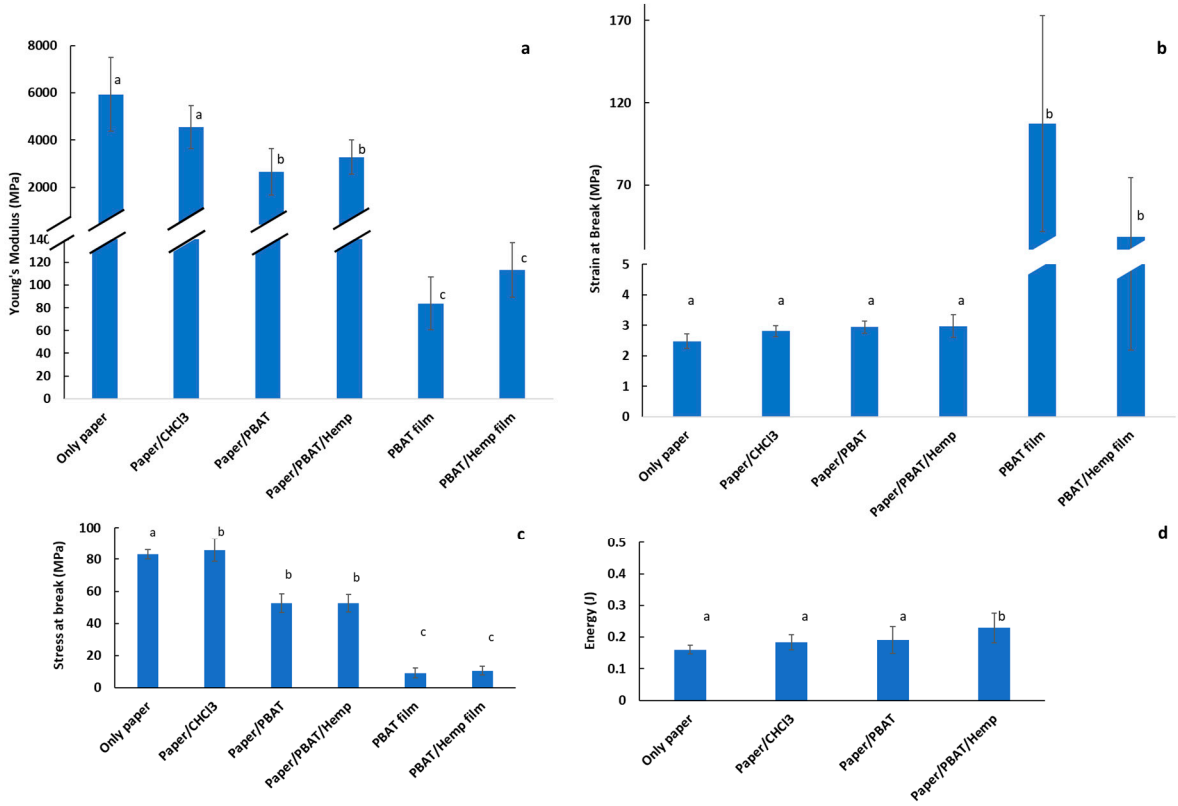

Figure 6. Mechanical properties of PBAT-based cast film and coated paper (different letters above columns indicate statistical differences). (**a**) Young´s Modulus; (**b**) Strain at break; (**c**) Stress at break; (**d**) Energy. Different letters above columns indicate statistic differences.

3.2.5. Optical Properties

Since the colour and opacity of the films could affect their performance in food applications, these parameters were also studied. Figure 7 presents the RGB colours calculated from the measured L*a*b* values for the several samples tested. The original data is presented in the Supplementary Information (Table S2).

As expected, a chromatic change was observed after the incorporation of hemp fibres into the PBAT matrix and an increase in the opacity from 57 to 79% was observed for the cast films. The opacity of the uncoated paper was high, with values between 80 and 90%, and was not affected by the coating with PBAT or PBAT with hemp incorporated, as expected, given the opacity of the paper.

3.2.6. Compostability Test

The compostability of the PBAT film and of PBAT-based coated paper was determined by monitoring the weight loss experienced in samples buried in fertile soil at 60 °C and 65% RH. PBAT degrades either through the transformation of carbon to volatile carbon dioxide and/or incorporation of soil microorganisms into their biomass [52]. Figure 8 presents the data obtained from the compostability test represented as the materials' weight loss in percentage over the time of exposure to the soil. After eight weeks, the weight loss of PBAT/hemp films was ca. 50%, while the weight loss of PBAT films without hemp was only ca. 25%. Similar results were observed for the weight loss of paper coated with PBAT/hemp, which was as much as 10 times higher than the paper coated with PBAT only, showing that the hemp fibres enhance significantly the compostability of PBAT films.

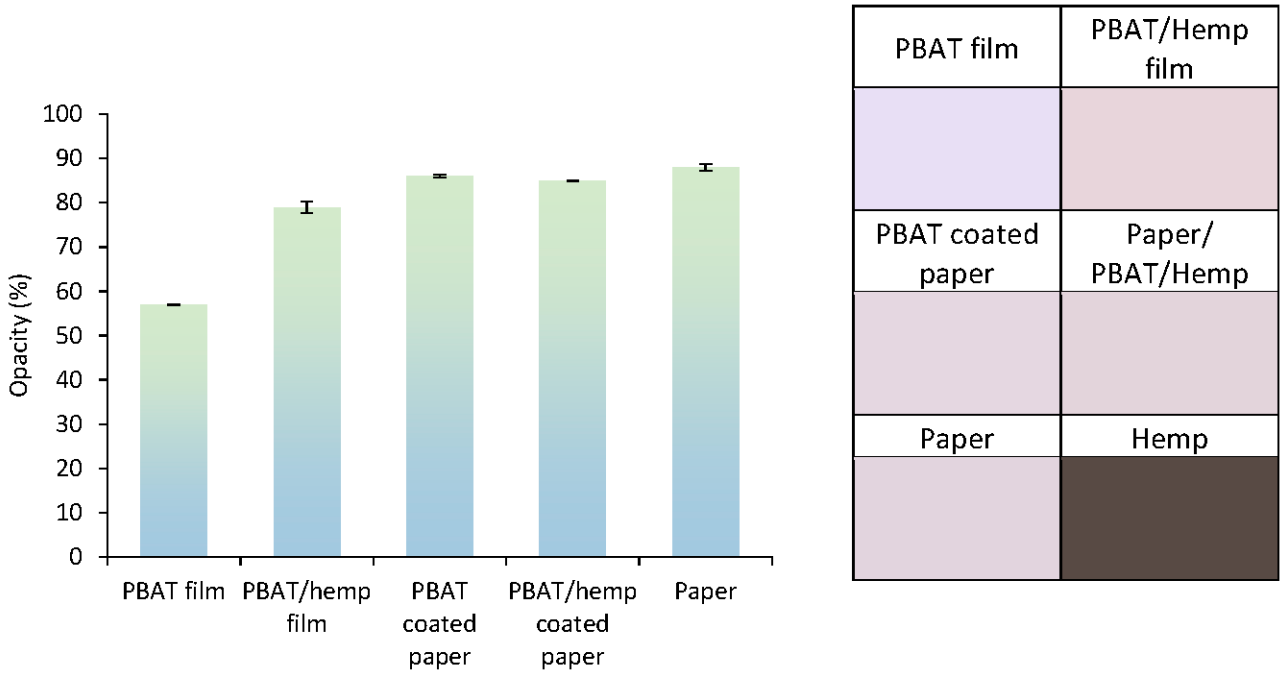

Figure 7. Opacity and colour of PBAT cast film and coated paper (neat or with hemp incorporation).

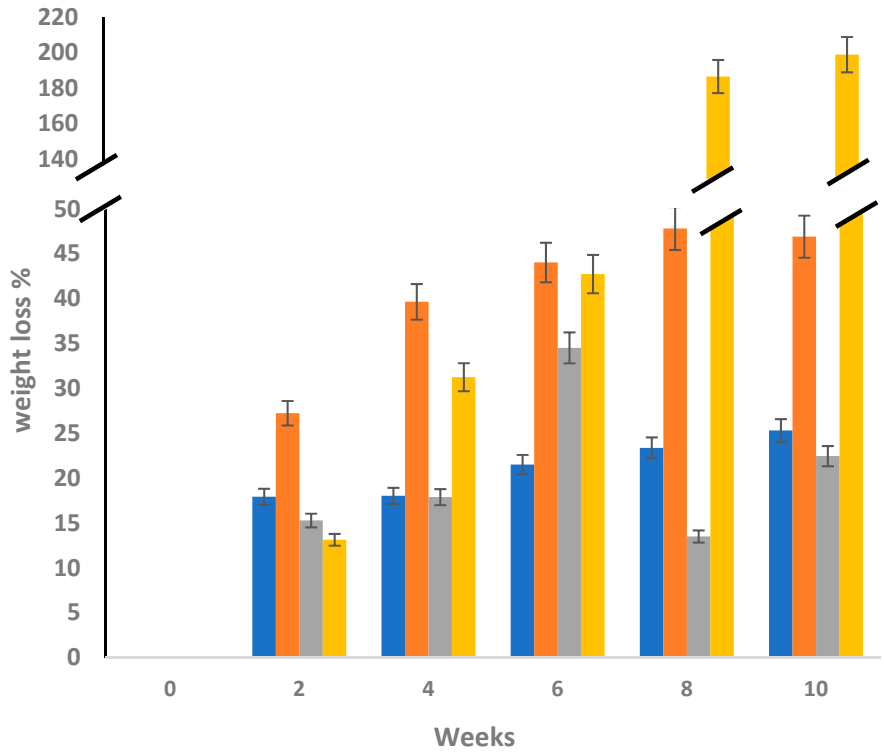

Figure 8. Weight loss during composting (PBAT film, PBAT/hemp film, Paper/PBAT, and Paper/PBAT/hemp).

The kinetics of the weight loss of materials without hemp (PBAT film and paper/PBAT) were similar to each other up to 10 weeks, presenting a value of ca. 25%, although significantly different values ($p < 0.05$) were found at 6 and 8 weeks. The behaviour trend for the materials incorporated with hemp was also similar to each other (although at different levels, $p < 0.05$), and for both materials, the weight loss occurred faster at earlier times of

composting (when compared with the materials without hemp) and the degradation rate slowed down at longer times of composting.

The morphology of the samples under degradation was observed by SEM. Figures 9a and 9b show the SEM images of the degraded films of pure PBAT and PBAT/hemp, respectively. In the pure PBAT films, slight surface damage was observed in the second week, and large cracks became apparent in the fourth week. The degradation became deeper and bigger in the sixth week. The progress of the PBAT/hemp-film composting starts with the erosion of the surface, justified by the presence of micro-holes as discussed before, which allows the microorganisms to access the bulk of the materials, creating large, damaged zones, particularly after the 8th week, in agreement with the weight loss recorded.

a

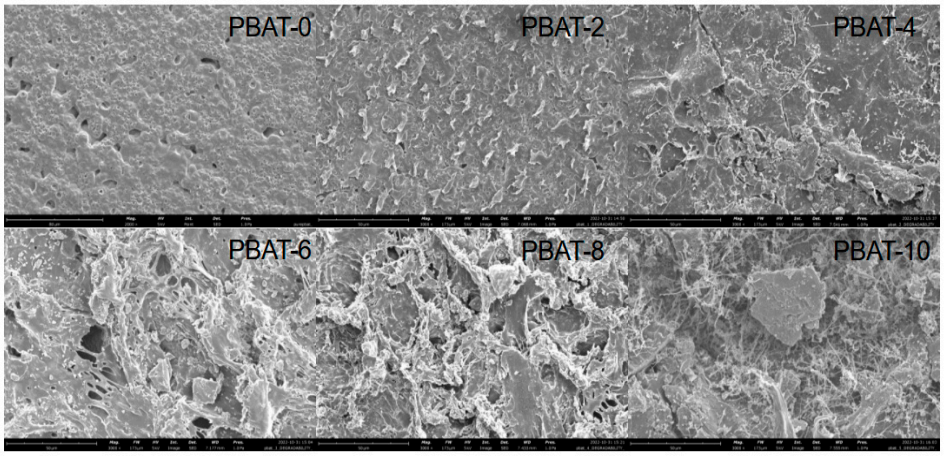

b

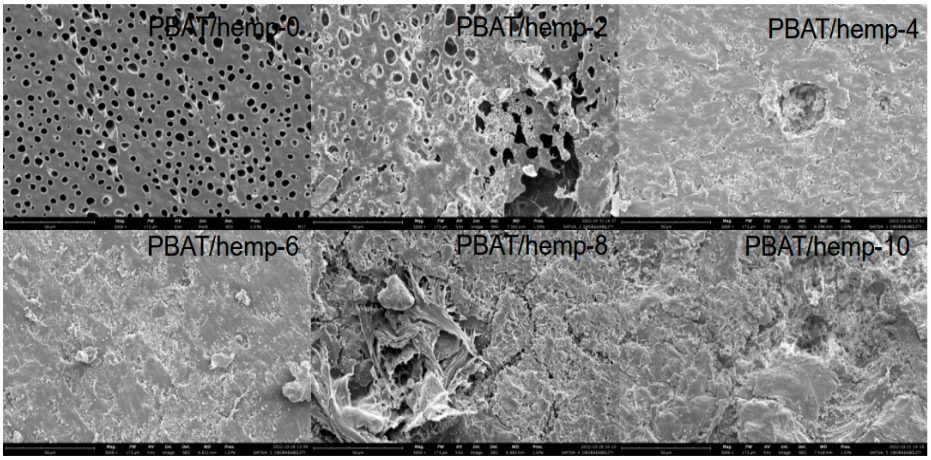

Figure 9. SEM images of degraded cast films: (**a**) PBAT and (**b**) PBAT/hemp-X (where X indicates the sampling week).

The thermal transitions for the PBAT and PBAT/hemp under degradation were analysed by DSC. The thermograms do not present any differences for the glass transition and melting temperatures. There was an increase in the crystallisation temperature (Tc) with the increasing time of composting. The Tc of PBAT/hemp is 63.3 °C, and during the degradation process, it goes up to 79.0 °C after 2 weeks and 84.0 °C after 10 weeks, on average. Similarly, the Tc of pure PBAT increases upon degradation. These results agree with results published in the literature for a PBAT blend with PLA (50% PBAT) that showed an increase from 66.4 to 68.2 °C [53]. Upon degradation, the amorphous region degrades faster, increasing the relative crystallinity [54], therefore yielding higher Tc. The thermograms for the cooling cycles of the samples are presented in the Supplementary Information (Figure S2).

The FTIR spectra of the samples under composting were determined (Figure 10) and may be compared with that of hemp and PBAT. The FTIR spectrum of hemp fibre is presented in Figure 10a, and absorption bands were identified according to [46]; namely, bands between 1312 cm^{-1} and 1465 cm^{-1} corresponding to cellulose and hemicellulose; stretching vibration of hydroxyl groups and symmetric and asymmetric stretching vibrations of the C–H group of cellulose at 3380 cm^{-1}, 2903 cm^{-1}, and 2937 cm^{-1}, respectively; spectra ranging from 881 cm^{-1} to 1168 cm^{-1} corresponding to the backbone structure of cellulose and hemicellulose; lignin aromatic-ring stretching at approximately 1600–1500 cm^{-1}; carboxylic functional groups (C=O) at 1744 cm^{-1}; and (C–O) at 1250 cm^{-1} of pectin and wax were recorded. The main bands observed for PBAT are those corresponding to the asymmetrical stretch of CH_2 (2956 cm^{-1}), stretching vibration of C=O (1710 cm^{-1}), skeleton vibration of the benzene ring (1504 cm^{-1}), trans-CH_2-plane bending vibration (1410 and 1386 cm^{-1}), symmetric stretching vibration of C-O (1268 cm^{-1}), C-O left–right symmetric stretching vibration absorption (1164 cm^{-1}), bending vibration absorption at the surface of adjacent hydrogen atoms on the phenyl ring (1018 cm^{-1}), trans-C-O symmetric stretching vibration (934 cm^{-1}), and bending vibration absorption of the C-H plane of the benzene ring (728 cm^{-1}).

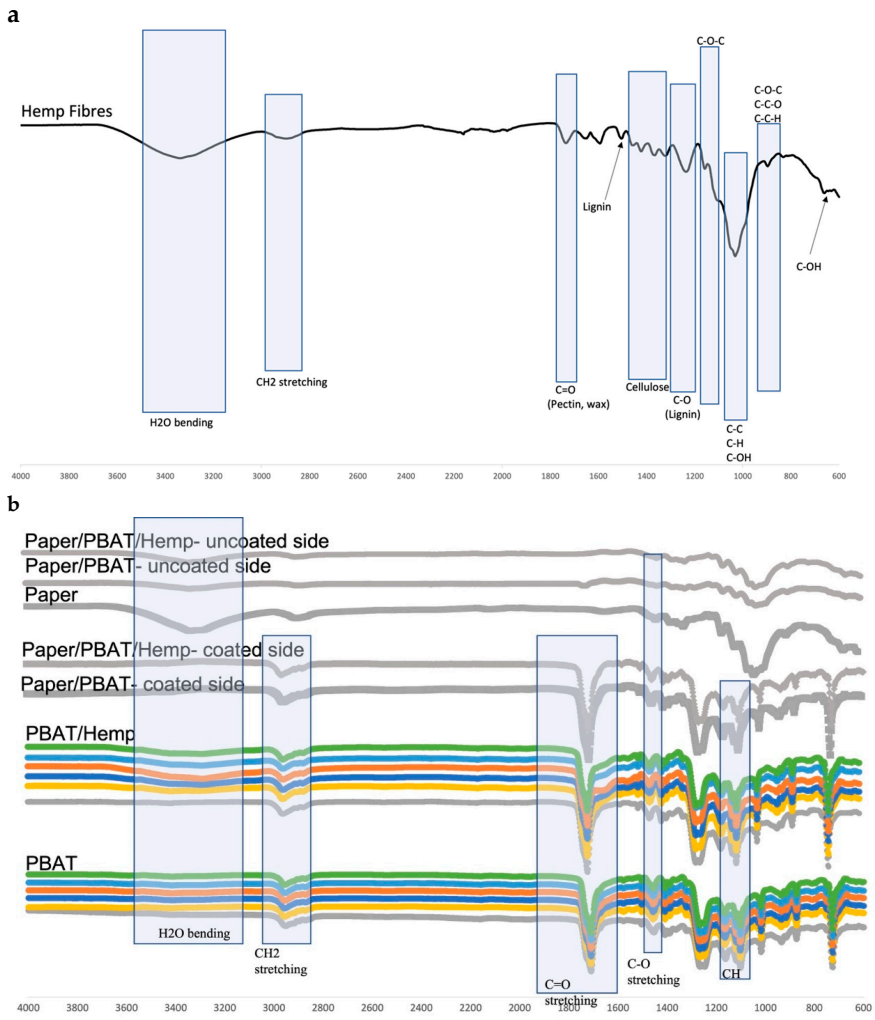

Figure 10. (**a**) FTIR of hemp fibre; (**b**) FTIR of PBAT and PBAT/hemp films, coated side of paper, uncoated side of paper, and pure paper (—0, —2, —4, —6, —8, —10 weeks of degradation.

The PBAT film does not present a water absorption band, whereas the addition of hemp fibres makes the band apparent. In composting samples, this water band in the PBAT/hemp film further increases with time, indicating the presence of moisture, thus proving degradation. Paper coated with PBAT shows a remarkable decrease in the band,

which is in agreement with the data from the WVP, and a slight increase is noticed when paper is coated with the PBAT/hemp film. The main bands of the materials did not change over the composting time, which has been previously reported for PBAT-based materials [55].

4. Conclusions

Hemp fibres from industry residues were incorporated into PBAT, and films were produced via casting. The combined PBAT/hemp can be applied to coat paper, resulting in improved properties with regard to moisture barriers, mechanical properties, and compostability. The study was conducted with reference to PBAT films. The water vapour permeability of PBAT increased slightly in the presence of hemp fibres, as expected. Regarding the mechanical properties, the PBAT/hemp film is less stretchable but stronger than the pure PBAT. The influence of hemp fibres was significant on the compostability of the film, and the PBAT/hemp films were shown to be twice more compostable than the pure PBAT. Active properties of the films were not evaluated, but results on the chemical composition of the hemp showed that the stalk residues (a less noble part of the plant) still have the potential for antimicrobial and antioxidant properties. Therefore, these films and coatings are good candidates for active food packaging applications. This aspect should be further explored, considering the results obtained for the chemical analysis of the films, with tests to evaluate the antimicrobial and antioxidant properties: first, with *in vitro* experiments to screen the microbial agents sensitive to the effect of the hemp substances, and then *in situ*, with selected foods, for example, fresh-cut fruits and vegetables.

Supplementary Materials: The following supporting information can be downloaded at: https://www.mdpi.com/article/10.3390/coatings13071195/s1, Table S1: Compounds detected by GC-MS on hemp (HS, SPME, Liquid-Ethanol, Isoctane, Hexane/acetone mixture); Table S2: Optical properties of the materials: L*ab values; Figure S1: SEM image PBAT/hemp casted film (center of the film); Figure S2: Thermogram of the cooling cycles of cast films at different times of degradation.

Author Contributions: Conceptualization, F.P., H.L. and S.S.; methodology, F.P., H.L., S.S. and J.P.; validation, F.P.; formal analysis, H.L., S.S. and J.P.; investigation, H.L., S.S. and J.P.; resources, F.P.; data curation, H.L. and S.S.; writing—original draft preparation, H.L. and S.S.; writing—review and editing, F.P.; supervision, F.P.; funding acquisition, F.P. All authors have read and agreed to the published version of the manuscript.

Funding: This article/publication is based upon work co-financed by Fundo Europeu de Desenvolvimento Regional (FEDER) through the Programa Operacional Competitividade e Internacionalização (POCI), under the scope of the project BIOPROTECT—POCI-01-0247-FEDER-069858.

Institutional Review Board Statement: Not applicable.

Informed Consent Statement: Not applicable.

Data Availability Statement: All data that support the findings of this study are included within the article.

Conflicts of Interest: The authors declare no conflict of interest.

References

1. Promhuad, K.; Srisa, A.; San, H.; Laorenza, Y.; Wongphan, P.; Sodsai, J.; Tansin, K.; Phromphen, P.; Chartvivatpornchai, N.; Ngoenchai, P.; et al. Applications of Hemp Polymers and Extracts in Food, Textile and Packaging: A Review. *Polymers* **2022**, *14*, 4274. [CrossRef] [PubMed]
2. Manaia, J.P.; Manaia, A.T.; Rodriges, L. Industrial Hemp Fibers: An Overview. *Fibers* **2019**, *7*, 106. [CrossRef]
3. Khan, B.A.; Wang, J.; Warner, P.; Wang, H. Antibacterial properties of hemp hurd powder against *E. coli*. *J. Appl. Polym. Sci.* **2015**, *132*, 41588/1–41588/6. [CrossRef]
4. Plastics Europe. Plastics—The Facts 2019. An Analysis of European Plastics Production, Demand and Waste Data. 2016. Available online: https://plasticseurope.org/wp-content/uploads/2021/10/2019-Plastics-the-facts.pdf (accessed on 17 January 2023).
5. Silva, F.A.G.S.; Dourado, F.; Gama, M.; Poças, F. Nanocellulose Bio-Based Composites for Food Packaging. *Nanomaterials* **2020**, *10*, 2041. [CrossRef] [PubMed]

6. European Commission Press. Release Plastic Waste: A European Strategy to Protect the Planet, Defend Our Citizens and Empower Our Industries. 2018. Available online: https://ec.europa.eu/commission/presscorner/detail/en/IP_18_5 (accessed on 17 January 2023).
7. Ballesteros, L.F.; Lamsaf, H.; Sebastian, C.V.; Cerqueira, M.A.; Pastrana, L.; Teixeira, J.A. Active Packaging Systems Based on Metal and Metal Oxide Nanoparticles. In *Nanotechnology-Enhanced Food Packaging*; Wiley: Hoboken, NJ, USA, 2021. [CrossRef]
8. Jian, J.; Xiangbin, Z.; Xianbo, H. An overview on synthesis, properties and applications of poly(butylene-adipate-co-terephthalate)–PBAT. *Adv. Ind. Eng. Polym. Res.* **2020**, *3*, 19–26. [CrossRef]
9. Venkatesan, R.; Rajeswari, N. ZnO/PBAT nanocomposite films: Investigation on the mechanical and biological activity for food packaging. *Polym. Adv. Technol.* **2016**, *28*, 20–27. [CrossRef]
10. Pulikkalparambil, H.; Parameswaranpillai, J.; George, J.J.; Yorseng, K.; Siengchin, S. Physical and thermo-mechanical properties of bionano reinforced poly(butylene adipate-co-terephthalate), hemp/CNF/Ag-NPs composites. *AIMS Mater. Sci.* **2017**, *4*, 814–831. [CrossRef]
11. Venkatesan, R.; Rajeswari, N.; Tamilselvi, A. Antimicrobial, mechanical, barrier, and thermal properties of bio-based poly (butylene adipate-*co* -terephthalate) (PBAT)/Ag_2 O nanocomposite films for packaging application. *Polym. Adv. Technol.* **2017**, *29*, 61–68. [CrossRef]
12. Seligra, P.G.; Moura, L.E.; Famá, L.; Druzian, J.I.; Goyanes, S. Influence of incorporation of starch nanoparticles in PBAT/TPS composite films. *Polym. Int.* **2016**, *65*, 938–945. [CrossRef]
13. Kian, L.K.; Jawaid, M.; Mahmoud, M.H.; Saba, N.; Fouad, H.; Alothman, O.Y.; Karim, Z. PBAT/PBS Blends Membranes Filled with Nanocrystalline Cellulose for Heavy Metal Ion Separation. *J. Polym. Environ.* **2022**, *30*, 5263–5273. [CrossRef]
14. Phothisarattana, D.; Harnkarnsujarit, N. Migration, aggregations and thermal degradation behaviors of TiO_2 and ZnO incorporated PBAT/TPS nanocomposite blown films. *Food Packag. Shelf Life* **2022**, *33*, 100901. [CrossRef]
15. Laorenza, Y.; Harnkarnsujarit, N. Carvacrol, citral and α-terpineol essential oil incorporated biodegradable films for functional active packaging of Pacific white shrimp. *Food Chem.* **2021**, *363*, 130252. [CrossRef] [PubMed]
16. Leelaphiwat, P.; Pechprankan, C.; Siripho, P.; Bumbudsanpharoke, N.; Harnkarnsujarit, N. Effects of nisin and EDTA on morphology and properties of thermoplastic starch and PBAT biodegradable films for meat packaging. *Food Chem.* **2021**, *369*, 130956. [CrossRef] [PubMed]
17. Wangprasertkul, J.; Siriwattanapong, R.; Harnkarnsujarit, N. Antifungal packaging of sorbate and benzoate incorporated biodegradable films for fresh noodles. *Food Control.* **2020**, *123*, 107763. [CrossRef]
18. Olonisakin, K.; Wen, A.; He, S.; Lin, H.; Tao, W.; Chen, S.; Lin, W.; Li, R.; Zhang, X.-X.; Yang, W. The Development of Biodegradable PBAT-Lignin-Tannic Acid Composite Film: Properties, Biodegradability, and Potential Barrier Application in Food Packaging. *Food Bioprocess Technol.* **2023**, *16*, 1525–1540. [CrossRef]
19. Moustafa, H.; Guizani, C.; Dupont, C.; Martin, V.; Jeguirim, M.; Dufresne, A. Utilization of Torrefied Coffee Grounds as Reinforcing Agent To Produce High-Quality Biodegradable PBAT Composites for Food Packaging Applications. *ACS Sustain. Chem. Eng.* **2017**, *5*, 1906–1916. [CrossRef]
20. Mohanty, S.N.; Nayak, S.K. Biodegradable Nanocomposites of Poly(butylene adipate-co-terephthalate) (PBAT) and Organically Modified Layered Silicates. *J. Polym. Environ.* **2012**, *20*, 195–207. [CrossRef]
21. Fukushima, K.; Wu, M.-H.; Bocchini, S.; Rasyida, A.; Yang, M.-C. PBAT based nanocomposites for medical and industrial applications. *Mater. Sci. Eng. C* **2012**, *32*, 1331–1351. [CrossRef]
22. Correa, J.P.; Bacigalupe, A.; Maggi, J.; Eisenberg, P. Biodegradable PLA/PBAT/Clay Nanocomposites: Morphological, Rheological and Thermomechanical Behavior. *J. Renew. Mater.* **2016**, *4*, 258–265. [CrossRef]
23. Dhakal, H.; Zhang, Z.; Bennett, N. Influence of fibre treatment and glass fibre hybridisation on thermal degradation and surface energy characteristics of hemp/unsaturated polyester composites. *Compos. Part B Eng.* **2012**, *43*, 2757–2761. [CrossRef]
24. Panaitescu, D.M.; Nicolae, C.A.; Vuluga, Z.; Vitelaru, C.; Sanporean, C.G.; Zaharia, C.; Florea, D.; Vasilievici, G. Influence of hemp fibers with modified surface on polypropylene composites. *J. Ind. Eng. Chem.* **2016**, *37*, 137–146. [CrossRef]
25. Phongam, N.; Dangtungee, R.; Siengchin, S. Comparative Studies on the Mechanical Properties of Nonwoven- and Woven-Flax-Fiber-Reinforced Poly(Butylene Adipate-Co-Terephthalate)-Based Composite Laminates. *Polym. Mech.* **2015**, *51*, 17–24. [CrossRef]
26. Zeng, D.; Zhang, L.; Jin, S.; Zhang, Y.; Xu, C.; Zhou, K.; Lu, W. Mechanical Properties and Tensile Model of Hemp-Fiber-Reinforced Poly(butylene adipate-*co*-terephthalate) Composite. *Materials* **2022**, *15*, 2445. [CrossRef] [PubMed]
27. Marcuello, C.; Chabbert, B.; Berzin, F.; Bercu, N.B.; Molinari, M.; Aguié-Béghin, V. Influence of Surface Chemistry of Fiber and Lignocellulosic Materials on Adhesion Properties with Polybutylene Succinate at Nanoscale. *Materials* **2023**, *16*, 2440. [CrossRef] [PubMed]
28. Shorey, R.; Mekonnen, T.H. Sustainable paper coating with enhanced barrier properties based on esterified lignin and PBAT blend. *Int. J. Biol. Macromol.* **2022**, *209*, 472–484. [CrossRef]
29. Khwaldia, K.; Arab-Tehrany, E.; Desobry, S. Biopolymer Coatings on Paper Packaging Materials. *Compr. Rev. Food Sci. Food Saf.* **2009**, *9*, 82–91. [CrossRef]
30. Zang, X.; Jiang, Y.; Wang, X.; Wang, X.; Ji, J.; Xue, M. Highly sensitive pressure sensors based on conducting polymer-coated paper. *Sens. Actuators B Chem.* **2018**, *273*, 1195–1201. [CrossRef]

31. Mendes, T.P.P.; Pereira, I.; Ferreira, M.R.; Chaves, A.R.; Vaz, B.G. Molecularly imprinted polymer-coated paper as a substrate for highly sensitive analysis using paper spray mass spectrometry: Quantification of metabolites in urine. *Anal. Methods* **2017**, *9*, 6117–6123. [CrossRef]
32. Schneider, C.A.; Rasband, W.S.; Eliceiri, K.W. NIH Image to ImageJ: 25 Years of image analysis. *Nat. Methods* **2012**, *9*, 671–675. [CrossRef]
33. Tang, C.-H.; Ten, Z.; Wang, X.-S.; Yang, X.-Q. Physicochemical and Functional Properties of Hemp (*Cannabis sativa* L.) Protein Isolate. *J. Agric. Food Chem.* **2006**, *54*, 8945–8950. [CrossRef]
34. Mansor, A.M.; Lim, J.S.; Ani, F.N.; Hashim, H.; Ho, W.S. Characteristics of cellulose, hemicellulose and lignin of MD2 pineapple biomass. *Chem. Eng. Trans.* **2019**, *72*, 79–84. [CrossRef]
35. Casariego, A.; Souza, B.; Cerqueira, M.; Teixeira, J.; Cruz, L.; Díaz, R.; Vicente, A. Chitosan/clay films' properties as affected by biopolymer and clay micro/nanoparticles' concentrations. *Food Hydrocoll.* **2009**, *23*, 1895–1902. [CrossRef]
36. Liu, M.; Thygesen, A.; Summerscales, J.; Meyer, A.S. Targeted pre-treatment of hemp bast fibres for optimal performance in biocomposite materials: A review. *Ind. Crop. Prod.* **2017**, *108*, 660–683. [CrossRef]
37. Leizer, C.; Ribnicky, D.; Poulev, A.; Dushenkov, S.; Raskin, I. The Composition of Hemp Seed Oil and Its Potential as an Important Source of Nutrition. *J. Nutraceuticals Funct. Med. Foods* **2000**, *2*, 35–53. [CrossRef]
38. Ovidi, E.; Masci, V.L.; Taddei, A.R.; Torresi, J.; Tomassi, W.; Iannone, M.; Tiezzi, A.; Maggi, F.; Garzoli, S. Hemp (*Cannabis sativa* L., Kompolti cv.) and Hop (*Humulus lupulus* L., Chinook cv.) Essential Oil and Hydrolate: HS-GC-MS Chemical Investigation and Apoptotic Activity Evaluation. *Pharmaceuticals* **2022**, *15*, 976. [CrossRef]
39. Wiebelhaus, N.; Hamblin, D.; Kreitals, N.M.; Almirall, J.R. Differentiation of marijuana headspace volatiles from other plants and hemp products using capillary microextraction of volatiles (CMV) coupled to gas-chromatography–mass spectrometry (GC–MS). *Forensic Chem.* **2016**, *2*, 1–8. [CrossRef]
40. Exley, C.; Begum, A.; Woolley, M.P.; Bloor, R.N. Aluminum in Tobacco and Cannabis and Smoking-Related Disease. *Am. J. Med.* **2006**, *119*, 276.e9–276.e11. [CrossRef]
41. Fermo, P.; Soddu, G.; Miani, A.; Comite, V. Quantification of the Aluminum Content Leached into Foods Baked Using Aluminum Foil. *Int. J. Environ. Res. Public Health* **2020**, *17*, 8357. [CrossRef]
42. Stahl, T.; Taschan, H.; Brunn, H. Aluminium content of selected foods and food products. *Environ. Sci. Eur.* **2011**, *23*, 37. [CrossRef]
43. European Food Safety Authority (EFSA). Safety of aluminium from dietary intake—Scientific Opinion of the Panel on Food Additives, Flavourings, Processing Aids and Food Contact Materials (AFC). *EFSA J.* **2008**, *6*, 754. [CrossRef]
44. Shen, Z.; Rajabi-Abhari, A.; Oh, K.; Yang, G.; Youn, H.J.; Lee, H.L. Improving the Barrier Properties of Packaging Paper by Polyvinyl Alcohol Based Polymer Coating—Effect of the Base Paper and Nanoclay. *Polymers* **2021**, *13*, 1334. [CrossRef] [PubMed]
45. Pal, A.K.; Katiyar, V. Nanoamphiphilic Chitosan Dispersed Poly(lactic acid) Bionanocomposite Films with Improved Thermal, Mechanical, and Gas Barrier Properties. *Biomacromolecules* **2016**, *17*, 2603–2618. [CrossRef] [PubMed]
46. Gupta, A.; Chudasama, B.; Chang, B.P.; Mekonnen, T. Robust and sustainable PBAT—Hemp residue biocomposites: Reactive extrusion compatibilization and fabrication. *Compos. Sci. Technol.* **2021**, *215*, 109014. [CrossRef]
47. Stelea, L.; Filip, I.; Lisa, G.; Ichim, M.; Drobotă, M.; Sava, C.; Mureșan, A. Characterisation of Hemp Fibres Reinforced Composites Using Thermoplastic Polymers as Matrices. *Polymers* **2022**, *14*, 481. [CrossRef]
48. Cetin, M.S.; Aydogdu, R.B.; Toprakci, O.; Toprakci, H.A.K. Sustainable, Tree-Free, PLA Coated, Biodegradable, Barrier Papers from Kendir (Turkish Hemp). *J. Nat. Fibers* **2022**, *19*, 13802–13814. [CrossRef]
49. Bastarrachea, L.; Dhawan, S.; Sablani, S.S. Engineering Properties of Polymeric-Based Antimicrobial Films for Food Packaging: A Review. *Food Eng. Rev.* **2011**, *3*, 79–93. [CrossRef]
50. Zhang, Y.; Remadevi, R.; Hinestroza, J.P.; Wang, X.; Naebe, M. Transparent Ultraviolet (UV)-Shielding Films Made from Waste Hemp Hurd and Polyvinyl Alcohol (PVA). *Polymers* **2020**, *12*, 1190. [CrossRef]
51. Khwaldia, K.; Basta, A.H.; Aloui, H.; El-Saied, H. Chitosan–caseinate bilayer coatings for paper packaging materials. *Carbohydr. Polym.* **2014**, *99*, 508–516. [CrossRef]
52. Zumstein, M.T.; Schintlmeister, A.; Nelson, T.F.; Baumgartner, R.; Woebken, D.; Wagner, M.; Kohler, H.-P.E.; McNeill, K.; Sander, M. Biodegradation of synthetic polymers in soils: Tracking carbon into CO_2 and microbial biomass. *Sci. Adv.* **2018**, *4*, eaas9024. [CrossRef]
53. Ren, Y.; Hu, J.; Yang, M.; Weng, Y. Biodegradation Behavior of Poly (Lactic Acid) (PLA), Poly (Butylene Adipate-Co-Terephthalate) (PBAT), and Their Blends Under Digested Sludge Conditions. *J. Polym. Environ.* **2019**, *27*, 2784–2792. [CrossRef]
54. Fu, Y.; Wu, G.; Bian, X.; Zeng, J.; Weng, Y. Biodegradation Behavior of Poly(Butylene Adipate-Co-Terephthalate) (PBAT), Poly(Lactic Acid) (PLA), and Their Blend in Freshwater with Sediment. *Molecules* **2020**, *25*, 3946. [CrossRef] [PubMed]
55. Weng, Y.-X.; Jin, Y.-J.; Meng, Q.-Y.; Wang, L.; Zhang, M.; Wang, Y.-Z. Biodegradation behavior of poly(butylene adipate-co-terephthalate) (PBAT), poly(lactic acid) (PLA), and their blend under soil conditions. *Polym. Test.* **2013**, *32*, 918–926. [CrossRef]